

## Synthesis of High-quality Single-crystal Diamonds by Microwave Plasma Assisted Chemical Vapour Deposition

Pulkesh Prajapati<sup>1</sup>, Khyati Upadhyay<sup>1,2</sup>, Abhay Dasadia<sup>1\*</sup>, Vanaraj Solanki<sup>3</sup>

<sup>1</sup>AD Patel Institute of Technology, The CVM University, New Vallabh Vidyanagar-388121, Gujarat, India, <sup>2</sup>BN Patel Institute of Paramedical and Science, Sardar Patel University, Anand-388001, Gujarat, India, <sup>3</sup>Dr. KC Patel R and D Centre, Charotar University of Science and Technology (CHARUSAT), Changa, Anand-388421, Gujarat, India. \*Corresponding Author's Email: abhaydasadia@adit.ac.in

### Abstract

Microwave Plasma Assisted Chemical Vapor Deposition (MPACVD) is a prominent method for synthesizing high-quality single crystal diamonds under comparatively low pressure and temperature. The synthesis conditions were optimized using the MPACVD method, at substrate temperatures from 800 °C to 900 °C, with gas pressures in the range of 150–180 Torr and the volume concentrations of H<sub>2</sub> and CH<sub>4</sub> employed during deposition. The simultaneous changes in and analysis of the growth parameters enhanced the quality of the synthesized samples. An infrared pyrometer was utilized to determine the temperature of the substrate, while a mass flow controller regulated the flow rate of each gas. The application of the Low-Pressure High-Temperature (LPHT) process resulted in better-quality synthesized samples, as confirmed by Raman Spectroscopy as well High-Resolution X-Ray Diffraction (HRXRD). To confirm the diamond phase, Raman spectroscopy was utilized. HRXRD analysis was performed to evaluate the orientation of the crystallography phase in grown samples. The value of FWHM of the rocking curves in HRXRD reflects the quality of the homoepitaxial layer. The diamond crystals produced exhibit remarkable material characteristics that enable excellent performance in various applications, including medical diagnostics, radiation detection, optical components for laser windows in RF and microwave transmission, mechanical tools like cutting and brushing instruments and electrodes for electrochemical sensing.

**Keywords:** High Pressure, High Temperature, Microwave Plasma Assisted Chemical Vapor Deposition, Optical Properties, Single Crystal Diamond.

### Introduction

Single-crystal diamond has emerged as one of the most promising wide-bandgap semiconductor materials for next-generation electronic, photonic and quantum technologies. Owing to its exceptional combination of physical, thermal and electronic properties, diamond has attracted significant attention for high-power and high-frequency electronic devices capable of operating under extreme environmental conditions. In particular, diamond possesses an ultra-wide bandgap of approximately 5.47 eV, extremely high thermal conductivity exceeding 2000 W m<sup>-1</sup> K<sup>-1</sup>, high carrier mobility and a very large breakdown electric field (~10 MV cm<sup>-1</sup>). These properties enable efficient heat dissipation and stable device operation even under high temperature, high voltage and high radiation environments where conventional semiconductor materials such as silicon, silicon carbide and gallium nitride often encounter performance limitations (1–3). As a

result, diamond has been increasingly recognized as a key material platform for advanced power electronics, high-frequency devices and radiation-hard electronic systems.

In addition to its outstanding electronic characteristics, diamond also exhibits remarkable mechanical hardness, chemical stability and optical transparency across a wide spectral range extending from the ultraviolet to the infrared region. These properties make diamond particularly attractive for applications in optical windows, radiation detectors, high-performance heat spreaders and advanced photonic devices (4–5). However, the practical implementation of diamond in electronic and photonic systems requires extremely high crystalline quality and atomically smooth surfaces with minimal subsurface damage. Surface imperfections introduced during polishing or processing can significantly influence device reliability, carrier transport properties and optical

This is an Open Access article distributed under the terms of the Creative Commons Attribution CC BY license (<http://creativecommons.org/licenses/by/4.0/>), which permits unrestricted reuse, distribution and reproduction in any medium, provided the original work is properly cited.

(Received 06<sup>th</sup> November 2025; Accepted 15<sup>th</sup> April 2026; Published 30<sup>th</sup> April 2026)

performance. Therefore, the development of high-quality single-crystal diamond substrates with minimal defects and ultra-smooth surfaces remains an essential requirement for the successful integration of diamond into advanced device architectures.

Recent advances in diamond synthesis technologies have significantly improved the availability of high-quality single-crystal diamond substrates with reduced impurity concentrations and improved structural uniformity. These developments have accelerated research efforts focused on exploiting diamond for a wide range of emerging technological applications. In particular, single-crystal diamond has become a promising material platform for high-power electronic devices, high-frequency transistors, radiation-hard detectors and next-generation photonic systems (6).

Diamond synthesis is primarily achieved through two well-established techniques: High-Pressure High-Temperature (HPHT) synthesis and Chemical Vapour Deposition (CVD). The HPHT method replicates the natural geological conditions under which diamonds are formed deep within the Earth's mantle, typically requiring pressures exceeding 5 GPa and temperatures above 1500 °C (7). Although HPHT synthesis is widely used for producing gem-quality diamonds and industrial abrasives, the method offers limited control over impurity incorporation and crystal defects. In contrast, CVD techniques enable diamond growth under comparatively lower pressures while providing enhanced control over critical growth parameters such as gas composition, plasma density, microwave power and substrate temperature (8–10). Consequently, CVD techniques have become the preferred approach for producing high-purity single-crystal diamond materials suitable for electronic and optical applications.

Among the various CVD techniques, Microwave Plasma-Assisted Chemical Vapour Deposition (MPACVD) has emerged as one of the most widely adopted and reliable methods for synthesizing high-quality single-crystal diamond. In this technique, microwave plasma is used to activate a hydrogen-rich gas mixture containing a carbon precursor, typically methane. The plasma dissociates methane molecules and generates reactive carbon radicals that contribute to diamond growth on the substrate surface. Atomic

hydrogen present in the plasma plays a crucial role by selectively etching non-diamond carbon phases while stabilizing  $sp^3$ -bonded carbon structures, thereby promoting the formation of high-quality diamond films (11–13).

Despite the significant advantages offered by MPACVD, the synthesis of high-quality single-crystal diamond remains a complex process that is highly sensitive to growth parameters. During the growth process, undesirable graphitic ( $sp^2$ -bonded) carbon may form at the interface between the diamond substrate and the substrate holder. The formation of this graphitic layer can significantly increase the thermal contact resistance between the substrate and the holder, leading to non-uniform temperature distribution across the substrate surface. Such temperature gradients may adversely affect the growth kinetics and lead to the formation of structural defects, dislocations and non-diamond carbon phases, which ultimately degrade the crystalline quality of the grown diamond films (14–16).

In recent years, diamond has also attracted considerable attention in the rapidly developing field of quantum science and technology. The presence of optically active defects, commonly referred to as color centers, within the diamond lattice provides unique opportunities for quantum applications. Among these defects, the nitrogen-vacancy (NV) center has emerged as one of the most promising solid-state quantum systems due to its long spin coherence time and excellent optical addressability even at room temperature (17–19). NV centers enable highly sensitive detection of magnetic fields, temperature and electric fields at the nanoscale, making them ideal for applications in quantum sensing, nanoscale magnetometry and quantum information processing.

Chemical Vapour Deposition techniques provide significant flexibility in controlling diamond growth conditions, including substrate temperature, chamber pressure, microwave power and gas composition. By carefully optimizing these parameters, it is possible to significantly improve the structural quality, optical properties and growth stability of single-crystal diamond films (20).

In this study, the growth of single-crystal diamond using the MPACVD technique was systematically investigated by optimizing key synthesis

parameters, including substrate temperature, chamber pressure and gas composition. Understanding the relationship between these growth parameters and the resulting structural and optical properties is essential for improving the reproducibility and scalability of diamond synthesis. Such insights are expected to contribute to the development of high-quality diamond materials suitable for next-generation electronic, photonic and quantum technologies.

## Methodology

The experiments were carried out using a Seki Diamond MPACVD system (Model SDS 6K), operated at 2.45 GHz with a microwave power of 5–5.5 kW. The chamber was initially evacuated to a base pressure of  $\sim 1 \times 10^{-3}$  Torr prior to gas introduction. Commercially available single-crystal diamond (100)-oriented substrates ( $8 \times 8 \times 0.5$  mm<sup>3</sup>) were used as seed crystals. Before growth, the substrates were ultrasonically cleaned sequentially in acetone and isopropanol, followed by deionized water rinsing and nitrogen drying. In situ plasma pre-cleaning was then performed in hydrogen atmosphere at 20 Torr and 6 kW for 20 minutes to remove surface contaminants and non-diamond carbon. After pre-cleaning, the substrates were mounted on a molybdenum holder to ensure

good thermal contact. Hydrogen was introduced to generate a dense plasma under controlled temperature and pressure conditions. The gas flow rates were precisely regulated using mass flow controllers and the reactive gases were premixed prior to entering the reaction chamber to ensure uniform composition. Plasma density inside the chamber was monitored using optical emission spectroscopy (OES), while the substrate temperature was measured using an optical pyrometer. Two samples (D1 and D2), each with dimensions of  $8 \times 8 \times 0.5$  mm<sup>3</sup>, were synthesized by systematically optimizing gas flow rates and substrate temperature through an iterative trial-and-error approach. The growth was carried out at substrate temperatures ranging from 800–900 °C, gas pressures between 150–180 Torr and microwave power of 5–5.5 kW for a total growth duration of 98 hours. After growth, the samples were cooled gradually to room temperature under continuous hydrogen flow to minimize thermal stress. All growth parameters-including plasma density, substrate temperature, gas pressure and reactive gas concentration-play a critical role in achieving symmetric growth morphology and high crystalline quality.

The optimized growth parameters are summarized in Table 1.

**Table 1:** Summary of Growth Parameters

| Sample | Substrate Temperature (°C) | Gas Pressure (Torr) | Microwave Power (kW) | H <sub>2</sub> (sccm) | CH <sub>4</sub> (sccm) | N <sub>2</sub> (sccm) | Total Flow (sccm) | Growth Period (h) | Dimensions (mm) |
|--------|----------------------------|---------------------|----------------------|-----------------------|------------------------|-----------------------|-------------------|-------------------|-----------------|
| D1     | 800                        | 150                 | 5.5                  | 450                   | 30                     | 1                     | 481               | 98                | 8 × 8 × 1.8     |
| D2     | 900                        | 160                 | 5                    | 450                   | 40                     | 1                     | 491               | 98                | 8 × 8 × 1.8     |

The samples were annealed by this technique, where the H<sub>2</sub>/Ar plasma etching was carried out at 2000 °C and pressure 300 Torr. These conditions were applied to improve the structural quality and crystalline integrity of the synthesized diamonds using the Low-Pressure High-Temperature (LPHT)

technique, thereby suppressing graphitization during growth, as verified through Raman spectroscopy and High-Resolution X-ray Diffraction (HRXRD) analysis. Table 2 summarizes the selected stepwise heating schedule applied to the samples.

**Table 2:** LPHT Processing Conditions

| Substrate Temperature (°C) | Gas Pressure (Torr) | Time (Minutes) | H <sub>2</sub> (sccm) | Ar (sccm) | H <sub>2</sub> /Ar Ratio | Total Flow (sccm) |
|----------------------------|---------------------|----------------|-----------------------|-----------|--------------------------|-------------------|
| 1800–2000                  | 250–300             | 0–1            | 400                   | 100       | 4:1                      | 500               |
| 1500–1700                  | 200–250             | 1–30           | 400                   | 100       | 4:1                      | 500               |
| 1400–1600                  | 150–200             | 30–60          | 400                   | 100       | 4:1                      | 500               |

The LPHT treatment was performed under controlled temperature and pressure conditions with a constant hydrogen–argon gas mixture. Initially, the samples were exposed to temperatures of 1800–2000 °C at 250–300 Torr for 0–1 min, followed by intermediate processing at 1500–

1700 °C for 1–30 min. In the final stage, the temperature was gradually reduced to 1400–1600 °C with a processing duration of 30–60 min to stabilize the crystal structure. Throughout the process, a constant gas flow consisting of 400 sccm H<sub>2</sub> and 100 sccm Ar (H<sub>2</sub>/Ar ratio of 4:1) with a total

flow rate of 500 sccm was maintained. Significant alterations in the optical appearance of single crystal diamonds were observed after LPHT

treatment, as illustrated in Figures 1A, 1B, 2A and 2B.

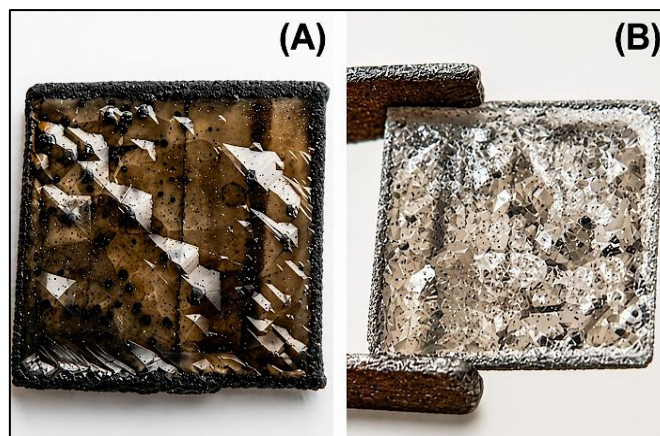


**Figure 1:** Sample D1: (A) Before LPHT Treatment, (B) After LPHT Treatment

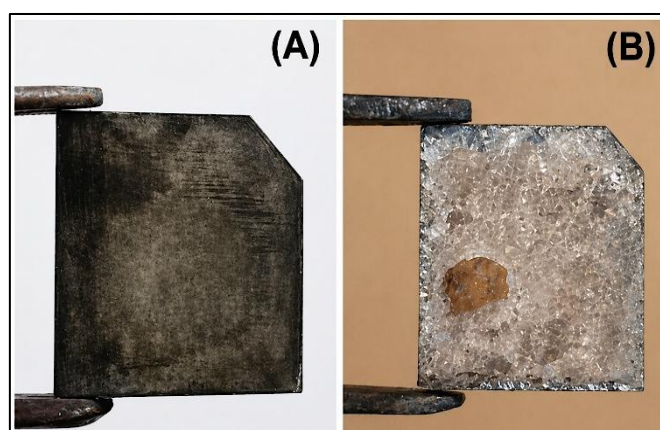


**Figure 2:** Sample D2: (A) Before LPHT Treatment, (B) After LPHT Treatment

## Results and Discussion

We observed the significant changes in optical property after LPHT treatment, which was quantified through different analytical method as under.

### High-Resolution X-Ray Diffraction (HRXRD)

HRXRD was utilized to investigate the surface morphology and quality of crystalline layer of the grown samples both before and after LPHT treatment. The method facilitates the assessment of extended defect density in epitaxial layers, where the Bragg peak FWHM from the  $\omega$ -scan correlates with the degree of extended defects in the layer (21-23). Crystal quality and the off-axis

angle orientations of substrate were examined. The measurements were performed using a D8 Discover from Bruker, Bangalore, operated at 40 kV and 40 mA using Cu K-alpha radiation. HRXRD was used to assess the surface structure and crystallinity of the layers by analyzing the rocking curves of the (100) reflections of the samples. For sample D1, the rocking curve was measured at  $59.61^\circ$  prior to LPHT treatment as given in Figure 3A and at  $59.12^\circ$  in Figure 3B afterward, indicating misorientations of  $0.61^\circ$  and  $0.12^\circ$  respectively. The peaks were fitted using a Gaussian function to determine the FWHM values.

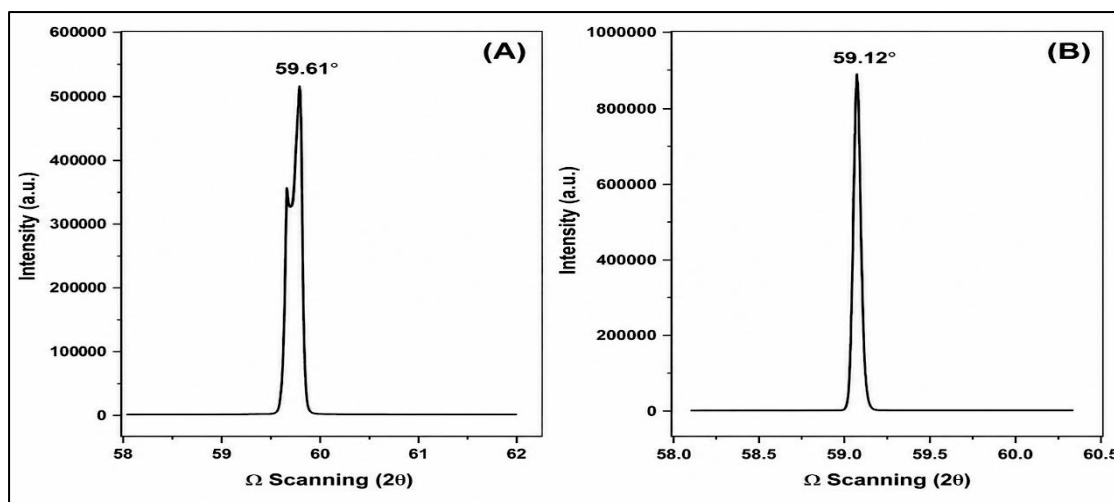


**Figure 3:** High-Resolution X-ray Diffraction (HRXRD)  $\omega$ -Scan Rocking Curves of Sample D1 recorded (A) Before LPHT Annealing showing a peak at 59.61° with a FWHM of 0.1497° and (B) After LPHT Annealing showing a peak at 59.12° with a Reduced FWHM of 0.038°

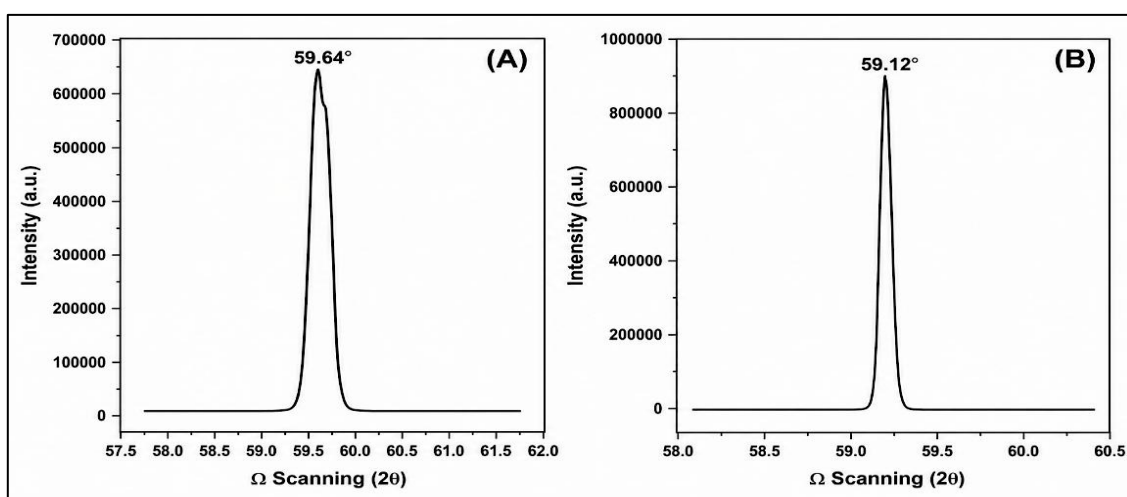


**Figure 4:** High-Resolution X-ray Diffraction (HRXRD)  $\omega$ -Scan Rocking Curves of Sample D2 recorded (A) Before LPHT Annealing showing a Diffraction peak at 59.64° with a FWHM of 0.1852° and (B) After LPHT Annealing exhibiting a peak at 59.12° with a Reduced FWHM of 0.043°

For the sample D2, we observed the rocking curve at 59.64° before the LPHT as depicted in Figure 4A, while after the LPHT the rocking curve observed at 59.12°, corresponding to misorientations of 0.64° and 0.12°, respectively, as depicted in Figure 4B. As shown in Figure 3B and Figure 4B, after LPHT treatment the samples exhibited smaller misorientation angles compared to before LPHT treatment, which demonstrated enhancement of crystals quality. After LPHT treatment the sample D1 exhibited the narrow FWHM value of 0.038° compare to before LPHT treatment higher FWHM value 0.1497°. Similarly, the sample D2 exhibited the smaller FWHM value of 0.043° compare to before LPHT treatment higher value of 0.1852°. A lower FWHM value indicated quality enhancement of grown samples after LPHT treatment (24, 25).

The observed reduction in rocking curve FWHM after LPHT processing indicates a significant improvement in the crystalline quality of the CVD-grown diamond layers. High-temperature treatment is known to facilitate lattice relaxation and reduce structural defects such as dislocations and micro-strain within the crystal lattice. Similar improvements in HRXRD peak narrowing have been reported for thermally treated diamond samples, confirming that post-growth thermal processing plays a critical role in enhancing structural perfection and reducing defect density in single-crystal diamond materials (12-14).

#### Raman spectroscopy

Raman Spectroscopy was performed on the obtained two samples to check the quality of crystal, assess internal stress and defects of the

structure both before and after LPHT treatment. The spectra were fitted using a Gaussian function to determine peak positions and assess crystalline

quality. Sometimes, the Raman spectra are greatly affected by the wavelength of the laser employed for excitation.

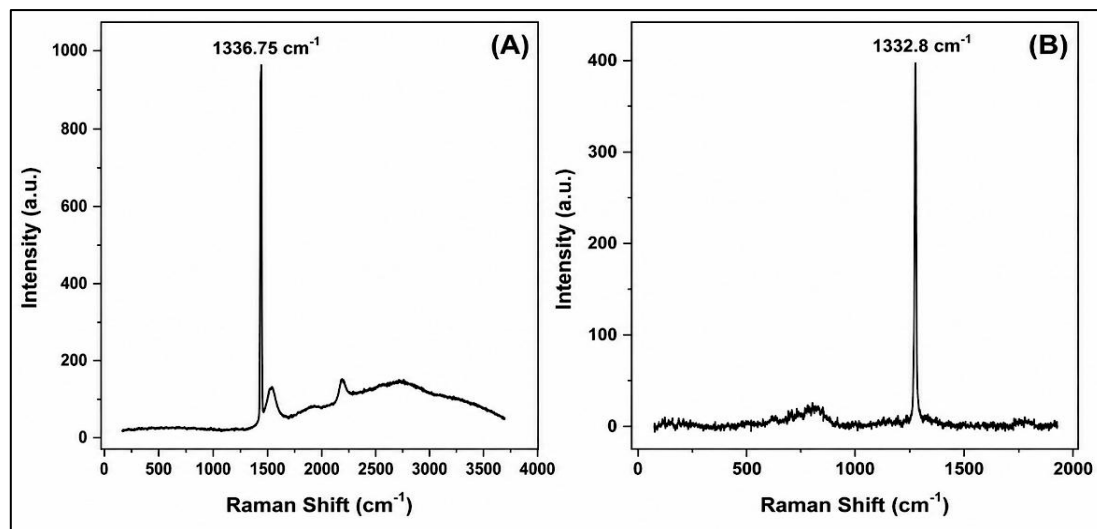


**Figure 5:** Raman Spectra of Sample D1 recorded (A) Prior to LPHT Annealing, showing a Broadened Peak Centred at  $1336.75 \text{ cm}^{-1}$  along with Additional Disorder-Related Features and (B) After LPHT Annealing, exhibiting a Sharp Diamond Characteristic peak at  $1332.8 \text{ cm}^{-1}$  with Significantly Reduced Background Intensity

In Figure 5A, Raman peak with increased broadening appears at  $1336.75 \text{ cm}^{-1}$  was observed with excited laser  $532 \text{ nm}$  before the LPHT treatment of sample D1 while the sharp Raman peak was observed at  $1332.8 \text{ cm}^{-1}$  with the same excitation laser as illustrated in Figure 5B after LPHT treatment. After LPHT annealing, the Raman spectrum exhibits a sharp diamond characteristic peak at  $1332.8 \text{ cm}^{-1}$  with a full width at half maximum (FWHM) of  $\sim 3.5 \text{ cm}^{-1}$ , indicating

improved crystalline quality compared to the as-grown sample, which showed a broadened peak centered at  $1336.75 \text{ cm}^{-1}$  (FWHM  $\sim 8\text{--}10 \text{ cm}^{-1}$ ). The peak intensity ratio ( $I_{1332}/I_{\text{background}}$ ) increased significantly after LPHT treatment, confirming enhanced phase purity. No detectable  $\text{sp}^2$  carbon-related G-band ( $\sim 1580 \text{ cm}^{-1}$ ) was observed after annealing, indicating effective suppression of graphitic carbon (26-29).

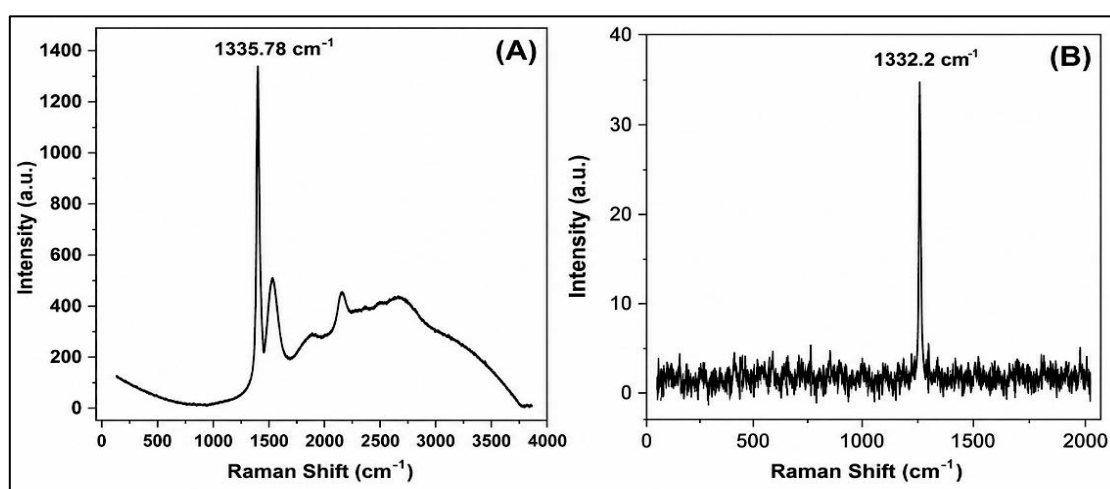


**Figure 6:** Raman Spectra of Sample D2 Recorded: (A) Prior to Annealing showing a Broadened Peak Centered at  $1335.78 \text{ cm}^{-1}$  along with Additional Disorder-Related Features and (B) After LPHT Annealing, exhibiting a Sharp Diamond Characteristic Peak at  $1332.2 \text{ cm}^{-1}$  with Significantly Reduced Background Intensity

Similarly, as shown in Figure 6A, Sample D2 displayed a broadened diamond peak at 1335.78  $\text{cm}^{-1}$  before annealing. After LPHT treatment, the peak shifted to 1332.2  $\text{cm}^{-1}$  with a reduced FWHM of  $\sim 3\text{--}4 \text{ cm}^{-1}$ , confirming substantial improvement in lattice ordering, as shown in Figure 6B. For example, internal strains can cause the Raman line to shift, while defects and impurities can cause new lines to appear in the spectrum. Raman peak broadening corresponds to random stress, whereas line shifts or splitting suggest directional stress. In addition, the crystal may include both amorphous  $\text{sp}^2$ -bonded carbon and  $\text{sp}^3$ -bonded carbon. The Raman peak at 1332  $\text{cm}^{-1}$  is characteristic of  $\text{sp}^3$  bonding (30-32).

## Conclusion

The Low-Pressure High-Temperature (LPHT) treatment significantly improves the crystalline quality of the synthesized diamond samples. High-resolution X-ray diffraction (HRXRD)  $\omega$ -scan rocking curve analysis revealed a substantial reduction in full width at half maximum (FWHM) after LPHT annealing. For Sample D1, the FWHM decreased from  $0.1497^\circ$  to  $0.038^\circ$ , while for Sample D2, it reduced from  $0.1852^\circ$  to  $0.043^\circ$ , indicating enhanced crystallinity and reduced structural disorder. The narrowing of the rocking curve peaks confirms improved lattice perfection and reduced mosaic spread following LPHT treatment.

Additionally, Raman spectra clearly demonstrate that LPHT treatment significantly improves the crystalline quality of both samples. After annealing, the diamond characteristic peak shifts toward  $\sim 1332 \text{ cm}^{-1}$  and becomes markedly sharper, indicating reduced lattice disorder. The narrowing of the Raman peak confirms improved structural ordering and reduced defect density. Moreover, the absence of a noticeable  $\text{sp}^2$  carbon G-band ( $\sim 1580 \text{ cm}^{-1}$ ) after LPHT treatment suggests effective suppression of graphitic phases and enhanced phase purity. The enhanced optical clarity and structural perfection make the single crystal diamonds highly suitable for advanced optical windows, high-power laser systems, radiation detectors and electronic and quantum sensing applications.

## Abbreviations

Ar: Argon,  $\text{CH}_4$ : Methane, CVD: Chemical Vapour Deposition, FWHM: Full Width at Half Maximum,

$\text{H}_2$ : Hydrogen, HPHT: High Pressure High Temperature, HRXRD: High Resolution X-Ray Diffraction, LPHT: Low Pressure High Temperature.

## Acknowledgement

The authors acknowledge the support of the Sophisticated Instrumentation Centre for Applied Research and Testing (SICART), Vallabh Vidyanaagar, Gujarat and thank Bruker, Bangalore, for providing access to their equipment for optical studies of the grown SCDs. They also appreciate the assistance of ABD Diamonds Pvt. Ltd., GIDC, Vatva, Ahmedabad, for their help in enabling the experimental studies on growth of single crystal diamond.

## Author Contributions

Abhay Dasadia: validation, supervision, review, editing, Pulkesh Prajapati: investigation, methodology, validation, formal analysis, Khyati Upadhyay: data curation, formal analysis, Vanaraj Solanki: review, editing.

## Conflict of Interest

The authors declare that they have no known competing financial interests or personal relationships that could have appeared to influence the work reported in this paper.

## Data Availability

All relevant data supporting the conclusions of this study are included within the manuscript.

## Declaration of Generative AI and AI Assisted Technologies in the Writing Process

The authors declare that the research concept, data and manuscript writing are original and not AI-generated. The use of AI tools was strictly limited to Grammarly for English language and grammar refinement. The authors take full responsibility for the content.

## Ethics Approval

This work focused on material synthesis and characterizations and does not involve any research with human participants or animals; therefore, ethics approval was not required.

## Funding

This research did not receive any specific grant from funding agencies in the public, commercial, or not-for-profit sectors.

## References

1. Wort CJH, Balmer RS. Diamond as an electronic material. *Materials Today*. 2008;11(1-2):22-28. doi:10.1016/S1369-7021(07)70349-8
2. Isberg J, Hammersberg J, Johansson E, *et al*. High carrier mobility in single-crystal plasma-deposited diamond. *Science*. 2002;297(5587):1670-1672. doi:10.1126/science.1074374
3. Baliga BJ. *Fundamentals of power semiconductor devices*. New York: Springer; 2008. ISBN 978-3-319-93987-2 ISBN 978-3-319-93988-9 (eBook). <https://doi.org/10.1007/978-3-319-93988-9>
4. May PW. Diamond thin films: A 21st-century material. *Philosophical Transactions of the Royal Society A: Mathematical, Physical and Engineering Sciences*. 2000;358(1766):473-495. doi:10.1098/rsta.2000.0542
5. Butler JE, Sumant AV. The CVD of nano diamond materials. *Chemical Vapor Deposition*. 2008;14(7-8):145-160. <https://doi.org/10.1002/cvde.200700037>
6. Tallaire A, Achard J, Brinza O, Gicquel A. Homoepitaxial growth of single crystal diamond using CVD. *Diamond and Related Materials*. 2006;15(10):1700-1707. doi: 10.1016/j.diamond.2006.03.034
7. Bundy FP. Direct conversion of graphite to diamond in static pressure apparatus. *Journal of Chemical Physics*. 1963;38(3):631-643. <https://doi.org/10.1063/1.1733716>
8. Angus JC, Will H, Stanko WS. Growth of diamond seed crystals by vapor deposition. *Journal of Applied Physics*. 1968;39(6):2915-2922. doi:10.1063/1.1656693
9. Goodwin DG, Butler JE. Theory of diamond chemical vapor deposition. In: Prelas MA, Popovici G, Bigelow LK, editors. *Handbook of Industrial Diamonds and Diamond Films*. New York: Marcel Dekker; 1998. p. 527-581. <https://www.chm.bris.ac.uk/pt/diamond/pdf/jpcm21-364201.pdf>
10. Gicquel A, Hassouni K, Silva F, Achard J. CVD diamond films: from growth to applications. *Current Applied Physics*. 2001;1(6):479-496. [https://doi.org/10.1016/S1567-1739\(01\)00061-X](https://doi.org/10.1016/S1567-1739(01)00061-X)
11. Kamo M, Sato Y, Matsumoto S, Setaka N. Diamond synthesis from gas phase in microwave plasma. *Journal of Crystal Growth*. 1983;62(3):642-644. [https://doi.org/10.1016/0022-0248\(83\)90411-6](https://doi.org/10.1016/0022-0248(83)90411-6)
12. Achard J, Tallaire A, Silva F, Bonnin X, Brinza O, Gicquel A. High-quality single crystal diamond grown by CVD. *Journal of Crystal Growth*. 2007;301-302:72-77. [https://www.researchgate.net/publication/228889367\\_High\\_quality\\_MPACVD\\_diamond\\_single\\_crystal\\_growth\\_High\\_microwave\\_power\\_density\\_regime](https://www.researchgate.net/publication/228889367_High_quality_MPACVD_diamond_single_crystal_growth_High_microwave_power_density_regime)
13. Tallaire A, Achard J, Sussmann R. Growth of large single-crystal diamond by CVD. *Diamond and Related Materials*. 2014; 47:36-52. doi: 10.1016/j.crhy.2012.10.008
14. Silva F, Achard J, Tallaire A, Bonnin X, Brinza O, Gicquel A. Single crystal CVD diamond growth strategy by the use of a 3D geometrical model: Growth on (113) oriented substrates. *Diamond and Related Materials*. 2010;19(4):395-403. doi: 10.1016/j.diamond.2008.01.006
15. Yamada H, Chayahara A, Mokuno Y. Method to increase the thickness and quality of diamond layers using plasma chemical vapor deposition under (H, C, N, O) system. *Diamond and Related Materials*. 2012; 24:32-38. <https://doi.org/10.1016/j.diamond.2019.107652>
16. Achard J, Tallaire A, Gicquel A. Growth of large size diamond single crystals by plasma assisted chemical vapour deposition: Recent achievements and remaining challenges. *Journal of Crystal Growth*. 2005;284(3-4):396-405. <https://doi.org/10.1016/j.crhy.2012.10.008>
17. Doherty MW, Manson NB, Delaney P, Jelezko F, Wrachtrup J, Hollenberg LCL. The nitrogen-vacancy colour centre in diamond. *Physics Reports*. 2013;528(1):1-45. doi: 10.1016/j.physrep.2013.02.001
18. Schirhagl R, Chang K, Loretz M, Degen CL. Nitrogen-vacancy centers in diamond: nanoscale sensors for physics and biology. *Annual Review of Physical Chemistry*. 2014; 65:83-105. doi:10.1146/annurev-physchem-040513-103659
19. Rondin L, Tetienne JP, Hingant T, Roch JF, Maletinsky P, Jacques V. Magnetometry with nitrogen-vacancy defects in diamond. *Reports on Progress in Physics*. 2014;77(5):056503. doi:10.1088/0034-4885/77/5/056503
20. Collins AT. The Electronic and Optical Properties of Diamond; Do they Favour Device Applications? *Reports on Progress in Physics*. 1982;45(4):417-458. doi:10.1557/PROC-162-3
21. Gómez J. Surface morphology and spectroscopic features of homoepitaxial diamond films prepared by microwave plasma-assisted chemical vapor deposition at high methane concentrations. *Materials*. 2022;15(21):7416. doi:10.3390/ma15217416
22. Xiang X, Wang X, Peng Y, *et al*. Synthesis and characterization of high-quality {100} diamond single crystal. *Journal of Materials Science: Materials in Electronics*. 2017; 28:9813-9819. doi:10.1007/s10854-017-6735-7
23. Dychalska A, Fabisiak K, Paprocki K, Makowiecki J, Szybowicz M, Ossowski T. A Raman spectroscopy study of the effect of thermal treatment on structural and photoluminescence properties of CVD diamond films. *Materials & Design*. 2016; 109:532-539. doi: 10.1016/j.matdes.2016.09.092
24. Wang X, Duan P, Cao Z, *et al*. Surface morphology of the interface junction of CVD mosaic single-crystal diamond. *Materials*. 2019; 13:91. doi:10.3390/ma13010091
25. Praver S, Nemanich RJ. Raman spectroscopy of diamond and doped diamond. *Philosophical Transactions of the Royal Society A: Mathematical, Physical and Engineering Sciences*. 2004;362(1824): 2537-2565. doi:10.1098/rsta.2004.1451
26. Paprocki K, Adam DW, Marek T, *et al*. The comparative studies of HF CVD diamond films by Raman and XPS spectroscopies. *Diamond and Related Materials*. 2019; 98:107536. doi: 10.1016/j.diamond.2019.01.020

27. Zhu X, Liu J, Shao S, *et al.* Effect of LPHT annealing on interface characteristics between HPHT Ib diamond substrates and homoepitaxial CVD diamond layers. *Journal of Materials Research*. 2020;35(5):3123-3134. doi:10.1557/jmr.2019.407
28. Mao R, Cui X, Hao J, *et al.* Densification and surface carbon transformation of diamond during hot-pressing. *Materials*. 2024;17(3):603. doi:10.3390/ma17030603
29. Zhang S, Ye Z, Zhu Y, *et al.* Enhanced Optical Properties of CVD Diamond through HPHT Annealing. *Crystal Growth and Design*. 2024; 24(16). doi: 10.1016/j.diamond.2021.108269
30. Agar JW 3rd, Drory MD. Quantitative measurement of residual biaxial stress by Raman spectroscopy in diamond grown on a titanium alloy by chemical vapor deposition. *Physical Review B*. 1993;48(4):2601-2604. doi:10.1103/PhysRevB.48.2601
31. Fabisiak K. Orientation dependence of cathodoluminescence and photoluminescence spectroscopy of defects in chemical-vapor-deposited diamond microcrystal. *Materials*. 2020;13(23):5446. doi:10.3390/ma13235446
32. Ralchenko VG. Diamond deposition on steel with CVD tungsten intermediate layer. *Diamond and Related Materials*. 1995;4(5-6):754-758. doi:10.1016/0925-9635(94)05299-9

**How to Cite:** Prajapati P, Upadhyay K, Dasadia A, Solanki V. Synthesis of High-quality Single-crystal Diamonds by Microwave Plasma Assisted Chemical Vapour Deposition. *Int Res J Multidiscip Scope*. 2026;7(2): 1804-1812. DOI: 10.47857/irjms. 2026.v07i02.09043